The technique of MIEELDLD as a measure of the shock-capturing property of numerical methods for hyperbolic conservation laws

A.R Appadu[a,*], and SN Neossi Nguetchue[b]
[a, b,] Department of Mathematics and Applied Mathematics, University of Pretoria, Pretoria 0002, South Africa.
Corresponding author*; Email: Rao.Appadu@up.ac.za or biprao2@yahoo.com

Abstract
In this paper, we use some numerical methods namely Lax-Wendroff (LW), two-step Lax-Friedrichs (LF), two variants of composite methods made up of Lax-Wendroff and the two-step Lax-Friedrichs and Fromm's scheme to solve a 1D linear advection and 1D diffusionless Burger's equation, at some values of the Courant number. We then use two optimisation techniques based on both dispersion and dissipation and two optimisation techniques based on only dispersion and obtain the variation of the integrated errors vs the CFL number. It is seen that out of the five techniques, only one is a good measure of the shock-capturing of property of numerical methods.

Keywords:
composite; dispersion; dissipation; shock-capturing; optimisation.

1 Introduction

One of the common ways of measuring the relative merit of a numerical scheme for advection is to consider the scheme's dispersion and dissipation [20]. All linear numerical schemes are either dispersive or dissipative [24]. The two-step Lax-Friedrichs (LF) scheme is first order in time and space and is dissipative in regions of discontinuity while MacCormack (MC) scheme is second-order and therefore dispersive in nature i.e it generates oscillations in regions of discontinuity. This paper is devoted to the study of some numerical schemes when used to approximate the 1D linear advection equation and 1D diffusionless Burger's equation.
Work on scheme dispersion reduction was first reported by Fromm [10]. Fromm's scheme in 1D is made up of a linear combination of Lax-Wendroff (LW) and the Beam-Warming second-order upwind (BW) schemes as these two dispersive schemes have phase errors in opposite directions. The Lax-Wendroff scheme in 1D induces lagging phase error mostly and hence gives rise to pre-shock oscillations while the BW scheme in 1D causes leading phase error and thus generates post-shock oscillations. The Fromm's scheme in 1D is an improved scheme over both LW and BW schemes and is Total Variation Bounded when it is stable [15].
We can also combine dispersive and dissipative schemes to obtain composite schemes. This idea as pointed out by Len Margolin was implemented in meteorological codes which compose the oscillatory second order Leap-Frog scheme with the dissipative backward Euler scheme [13]. Kasahara and Washington [14] use a three-level Leap-Frog scheme for 50 time steps which is inherently unstable followed by one cycle of the Lax-Wendroff scheme. Liska and Wendroff have obtained a composite scheme which comprises of Lax-Wendroff or Corrected Lax-Friedrichs (CF) as the dispersive scheme and the two-step Lax-Friedrichs

(LF) scheme as the dissipative scheme to obtain the composite Lax-Wendroff/Lax-Friedrichs (LWLF) scheme or Corrected Lax- Friedrichs/Lax-Friedrichs scheme. This approach does not require a limiter and attains an adequate accuracy by adjusting the number of times of applying these two schemes i.e LW/CF and LF schemes which have counter remainder effects. They formulated various forms of the composite LWLF scheme as LWLFn schemes consisting of (n-1) applications of LW scheme and one application of the LF scheme. In a similar approach to [13], we have combined the dispersive MacCormack (MC) scheme with the dissipative 2-step Lax-Friedrichs scheme when used to discretise the 1D linear advection equation and 2D scalar advection equation to obtain the MCLFn schemes [1].
In a recent work [3], a composite scheme has been constructed by using a linear combination of MacCormack and the two-step Lax-Friedrichs scheme for the 1D linear advection equation. For optimal shock-capturing, the ratio of MC:LF has been found to be $0.66 : 0.34$.

2 Organisation of paper

The paper is organised as follows. In section 3, we study the damping and dispersive characteristics of some numerical methods approximating the 1D linear advection equation. In section 4, we show how to quantify the errors from the numerical results into dissipation and dispersion errors by using a technique devised by Takacs [20]. Section 5 describes the two numerical experiments considered. In section 6, we consider some standard and composite schemes when used to discretise the 1D linear advection and 1D diffusionless Burger's equation. Sections 7 and 8 describe briefly some techniques of optimisation based on dispersion or both dispersion and dissipation and we obtain plots of the integrated errors vs the CFL number. In sections 9 and 10, we present the results when some schemes are used to solve propagation of the Boxcar function and 1D Burger's equation and compute some types of errors. Section 11 highlights the salient features of the paper.

3 Dispersive and Dissipative Characteristics of numerical methods

Dissipation is defined as the constant decrease with time of the amplitude of plane waves as they propagate in time. If the modulus of the amplification factor, denoted by AFM is equal to one, a disturbance neither grows nor damps [12]. The modulus of the amplification factor is also a measure of the stability of a scheme. If this value is greater than one, this creates instability while damping is present whenever this value is less then one [16]. When the modulus of the amplification factor exceeds one, this indicates an unstable mode [7].
The relative phase error (RPE) is a measure of the dispersive character of a scheme. This quantity is a ratio and measures the velocity of the computed waves to that of the physical waves.
If the RPE is greater than one, the computed waves appear to move faster than the physical waves [12] thus causing phase lead. A ratio less than one implies that the computed waves will move slower than the physical waves, causing phase lag.
We now obtain an expression for the RPE of a numerical scheme approximating the 1D linear advection equation which is given by

$$u_t + \beta u_x = 0. \tag{1}$$

A perturbation for u is

$$u = \exp(I\ (w_1\ t - \theta x)), \tag{2}$$

where t and x are time and space variables, θ is wavenumber and w_1 is the dispersion relation [19].
On using the perturbation for u into (1), we obtain the following equation,

$$I\ w_1 + \beta\ (-I\ \theta) = 0. \tag{3}$$

Hence the dispersion relation is given by

$$w_1 = \beta\ \theta. \tag{4}$$

The exact phase velocity is $\dfrac{\Re(w_1)}{\theta}$ which simplifies as β.
We now obtain the numerical phase velocity. We let the amplification factor of the scheme approximating Eq. (1) be

$$\xi = A + I\ B. \tag{5}$$

Then, we can write $\xi = \exp(-b\ k)$ [19] where b is the exponential growth rate and k is the temporal step size and we obtain

$$b = \frac{1}{k}\ \log\Big(\frac{A - I\ B}{A^2 + B^2}\Big). \tag{6}$$

The numerical phase velocity is computed as $\dfrac{\Im(b)}{\theta}$ and is equal to

$$-\frac{1}{k\ \theta}\tan^{-1}\Big(\frac{B}{A}\Big). \tag{7}$$

Since $k = \dfrac{r\ h}{\beta}$ and $w = \theta h$, the numerical phase velocity can be rewritten as

$$-\frac{\beta}{r\ w}\tan^{-1}\Big(\frac{B}{A}\Big). \tag{8}$$

The RPE is the ratio of the velocity of the computed waves to the velocity of the exact waves and is therefore equal to

$$-\frac{1}{r\ w}\tan^{-1}\Big(\frac{B}{A}\Big). \tag{9}$$

4 Quantification of errors from numerical results [20, 2, 4]

The Total Mean Square Error is calculated as

$$\frac{1}{N}\sum_{i=1}^{N}(u_i - v_i)^2,$$

where u_i represents the analytical solution and v_i, the numerical (discrete) solution at a given grid point, i.
The Total Mean Square Error can be expressed as

$$\frac{1}{N}\sum_{i=1}^{N}(u_i - v_i)^2 = \frac{1}{N}\sum_{i=1}^{N}(u_i)^2 + \frac{1}{N}\sum_{i=1}^{N}(v_i)^2 - \frac{2}{N}\sum_{i=1}^{N}u_i\ v_i. \tag{10}$$

Next,

$$\frac{1}{N}\sum_{i=1}^{N}(u_i-\overline{u})^2=\frac{1}{N}\sum_{i=1}^{N}\Big((u_i)^2-2u_i\ \overline{u}+(\overline{u})^2\Big) \tag{11}$$

and

$$\frac{1}{N}\sum_{i=1}^{N}(v_i-\overline{v})^2=\frac{1}{N}\sum_{i=1}^{N}\Big((v_i)^2-2v_i\ \overline{v}+(\overline{v})^2\Big). \tag{12}$$

The Total Mean Square Error can be further expressed as

$$\begin{aligned}\frac{1}{N}\sum_{i=1}^{N}(u_i-\overline{u})^2+\frac{1}{N}\sum_{i=1}^{N}(v_i-\overline{v})^2+\frac{2}{N}\sum_{i=1}^{N}u_i\ \overline{u}+\frac{2}{N}\sum_{i=1}^{N}v_i\ \overline{v}\\ -\frac{1}{N}\sum_{i=1}^{N}(\overline{u})^2-\frac{1}{N}\sum_{i=1}^{N}(\overline{v})^2-\frac{2}{N}\sum_{i=1}^{N}u_i\ v_i.\end{aligned} \tag{13}$$

The expression in (13) can be rewritten as

$$\sigma^2(u)+\sigma^2(v)+2(\bar{u})^2+2(\bar{v})^2-(\bar{u})^2-(\bar{v})^2-\frac{2}{N}\sum_{i=1}^{N}u_i\ v_i, \tag{14}$$

where $\sigma(u)$ and $\sigma(v)$ denote the variance of u and v respectively. $\overline{u}$ and $\overline{v}$ represent the means of u and v respectively.
Thus, the Total Mean Square Error is given by

$$\sigma^2(u)+\sigma^2(v)+\Big((\bar{u})^2-2\bar{u}\bar{v}+(\bar{v})^2\Big)+\Big(2\bar{u}\bar{v}-\frac{2}{N}\sum_{i=1}^{N}u_i\ v_i\Big) \tag{15}$$

which on further simplification yields

$$\sigma^2(u)+\sigma^2(v)+(\bar{u}-\bar{v})^2-2\Big(\frac{1}{N}\sum_{i=1}^{N}u_iv_i-\overline{u}\ \overline{v}\Big). \tag{16}$$

Thus, we have

$$\frac{1}{N}\sum_{i=1}^{N}(u_i-v_i)^2=\sigma^2(u)+\sigma^2(v)+(\bar{u}-\bar{v})^2-2\ Cov(u,v). \tag{17}$$

But, the correlation coefficient, ρ is given by $\dfrac{Cov(u,v)}{\sigma(u)\ \sigma(v)}$. Hence, the Total Mean Square Error can be written as

$$\frac{1}{N}\sum_{i=1}^{N}(u_i-v_i)^2=\sigma^2(u)+\sigma^2(v)+(\bar{u}-\bar{v})^2-2\ \rho\ \sigma(u)\ \sigma(v) \tag{18}$$

which simplifies to

$$\frac{1}{N}\sum_{i=1}^{N}(u_i-v_i)^2=(\sigma(u)-\sigma(v))^2+(\bar{u}-\bar{v})^2+2\ (1-\rho)\ \sigma(u)\ \sigma(v). \tag{19}$$

On putting $\rho=1$, we get $2\ (1-\rho)\ \sigma(u)\ \sigma(v)=0$. Thus, we define $(2\ (1-\rho)\sigma(u)\ \sigma(v))$ as the dispersion error since the correlation coefficient in statistics is analogous with phase lag or phase lead in Computational Fluid Dynamics.
Consequently, $(\sigma(u)-\sigma(u))^2+(\bar{u}-\bar{v})^2$ measures the dissipation error.

5 Numerical Experiment Considered

5.1 Problem I

The test problem we consider is the propagation of the Boxcar function [18] modelled by the equation,

$$u_t + u_x = 0. \tag{20}$$

This test problem involves discontinuous initial condition. The initial disturbance can be written as $g(x) = H(x+25) - H(x-25)$, for $-25 \leq x \leq 450$ where $H(x)$ is the Heaviside function which is a discontinuous function whose value is zero for negative argument and one for positive argument. It seldom matters what value is used for $H(0)$, since $H(x)$ is mostly used as a distribution.
The Fourier transformation of $g(x)$ consists of high frequency components. These need to be damped so as to avoid spurious high frequency waves. Hence, $g(x)$ can be used to study the effect of artificial damping [18].

5.2 Problem II

We solve the 1D diffusionless Burger's equation, $u_t + \left(\frac{1}{2}u^2\right)_x = 0$, for $x \in [-1, 1]$ at time, $T = 0.32$ with initial conditions being
$u(x, 0) = 1$ for $|x| < 1/3$,
$u(x, 0) = -1$ elsewhere.

At time, $T = 0.32$, the exact solution is given by [6, 17]

$$u(x, T) = \frac{1}{0.32}(x + 1/3),$$

if $x \geq -1/3 - 0.32$ and $x \leq 0.32 - 1/3$,

$$u(x, T) = 1.0,$$

if $x \geq 0.32 - 1/3$ and $x \leq 1/3$,
else

$$u(x, T) = -1.0.$$

6 Standard and Composite Schemes for 1D Linear Advection Equation and 1D Burger's equation

6.1 Lax-Wendroff Scheme

1D linear advection equation
The Lax-Wendroff scheme (LW) is a two-step second order explicit scheme much used in hyperbolic problems. The predictor and corrector steps are given by

$$u_{i+1/2}^{n+1/2} = \frac{1}{2}\,(u_{i+1}^n + u_i^n) - \frac{\beta k}{2h}(u_{i+1}^n - u_i^n), \tag{21}$$

and

$$u_i^{n+1} = u_i^n - \frac{\beta k}{h}(u_{i+1/2}^{n+1/2} - u_{i-1/2}^{n+1/2}). \tag{22}$$

However, it causes inevitable oscillations in those regions where shocks occur. A single expression for the LW scheme when applied to the 1D linear advection equation is given by

$$u_i^{n+1} = u_i^n - \frac{r}{2}(u_{i+1}^n - u_{i-1}^n) + \frac{r^2}{2}(u_{i+1}^n - 2u_i^n + u_{i-1}^n). \tag{23}$$

The MacCormack and Lax-Wendroff schemes are equivalent when used to discretise the 1D linear advection equation.
By using the Von Neumann analysis, we obtain the amplification factor of Lax-Wendroff scheme as

$$\xi_{LW} = 1 - 2\ r^2\ \sin^2\Big(\frac{w}{2}\Big) - Ir\sin(w). \tag{24}$$

For stability, the requirement is $|\xi_{LW}| \leq 1$. We obtain the region of stability as $0 < r \leq 1$.
The modified equation is given by

$$u_t + \beta u_x + \frac{1}{6}(\beta h^2 - \beta^3 k^2)\ u_{xxx} + \frac{1}{24}(\beta^2\ k\ h^2 - \beta^4 k^3)\ u_{xxxx} + ... = 0, \tag{25}$$

which indicates that the leading error terms are dispersive in nature.
The relative phase error is computed as

$$\frac{1}{r\ w}\tan^{-1}\Big(\frac{r\ \sin(w)}{1 - 2r^2\sin^2(w/2)}\Big). \tag{26}$$

1D Burger's equation
The predictor and corrector steps of Lax-Wendroff for the Burger's equation are

$$u_{i+1/2}^{n+1/2} = \frac{1}{2}\ \Big(u_{i+1}^n + u_i^n\Big) - \frac{k}{4\ h}\ \Big[(u_{i+1}^n)^2 - (u_i^n)^2\Big], \tag{27}$$

and

$$u_i^{n+1} = u_i^n - \frac{k}{2\ h}\ \Big[(u_{i+1/2}^{n+1/2})^2 - (u_{i-1/2}^{n+1/2})^2\Big], \tag{28}$$

respectively.

6.2 The Two-step Lax-Friedrichs

1D linear advection equation
The predictor and corrector steps of the two-step Lax-Friedrichs scheme are

$$u_{i+1/2}^{n+1/2} = \frac{1}{2}\ (u_i^n + u_{i+1}^n) - \frac{\beta k}{2h}(u_{i+1}^n - u_i^n), \tag{29}$$

and

$$u_i^{n+1} = \frac{1}{2}\ (u_{i-1/2}^{n+1/2} + u_{i+1/2}^{n+1/2}) - \frac{\beta k}{2h}\ (u_{i+1/2}^{n+1/2} - u_{i-1/2}^{n+1/2}). \tag{30}$$

A single expression for the Lax-Friedrichs scheme is [13]

$$u_i^{n+1} = \Big(\frac{1}{2} - \frac{r^2}{2}\Big)u_i^n + \Big(\frac{1}{4} - \frac{r}{2} + \frac{r^2}{4}\Big)u_{i+1}^n + \Big(\frac{1}{4} + \frac{r}{2} + \frac{r^2}{4}\Big)u_{i-1}^n. \tag{31}$$

The amplification factor is given by

$$\xi_{LF} = \frac{1}{2}\Big(1 + \cos(w) + r^2(\cos(w) - 1)\Big) - Ir\sin(w). \tag{32}$$

The region of stability satisfies the inequality $0 < r \leq 1$.

The relative phase error for the Lax-Friedrichs scheme is

$$RPE_{LF} = \frac{1}{rw} \tan^{-1}\Big(\frac{2r\sin(w)}{1+\cos(w)+r^2(\cos(w)-1)}\Big). \tag{33}$$

The modified equation is given by

$$u_t + \beta\ u_x + \Big(\frac{\beta^2 k}{4} - \frac{h^2}{4\ k}\Big)\ u_{xx} + \frac{1}{6}\ (-\beta^3 k^2 - \beta h^2)\ u_{xxx} + ... = 0, \tag{34}$$

and this indicates that the leading error terms are dissipative in nature.

Burger's equation

The predictor and corrector steps of Lax-Friedrichs scheme for the Burger's equation are

$$u_{i+1/2}^{n+1/2} = \frac{1}{2}\ (u_i^n + u_{i+1}^n) - \frac{k}{4h}\Big((u_{i+1}^n)^2 - (u_i^n)^2\Big), \tag{35}$$

and

$$u_i^{n+1} = \frac{1}{2}\ (u_{i-1/2}^{n+1/2} + u_{i+1/2}^{n+1/2}) - \frac{k}{4h}\ \Big[(u_{i+1/2}^{n+1/2})^2 - (u_{i-1/2}^{n+1/2})^2\Big]. \tag{36}$$

6.3 The Composite Lax-Wendroff/Lax-Friedrichs Scheme (LWLF2)

On combining one application of the Lax-Wendroff scheme with one application of the two-step Lax-Friedrichs scheme, we obtain the composite Lax-Wendroff/Lax-Friedrichs scheme (LWLF2) [13].
A single expression for the LWLF2 scheme is [1]

$$u_i^{n+2} = U11\ u_{i-2}^n + U22\ u_{i-1}^n + U33\ u_i^n + U44\ u_{i+1}^n + U55\ u_{i+2}^n, \tag{37}$$

where

$$U11 = \Big(\frac{1}{8}r + \frac{3}{8}r^2 + \frac{3}{8}r^3 + \frac{1}{8}r^4\Big), \tag{38}$$

$$U22 = \Big(\frac{1}{4} + \frac{3}{4}r + \frac{1}{4}r^2 - \frac{3}{4}r^3 - \frac{1}{2}r^4\Big), \tag{39}$$

$$U33 = \Big(\frac{1}{2} - \frac{5}{4}r^2 + \frac{3}{4}r^4\Big), \tag{40}$$

$$U44 = \Big(\frac{1}{4} - \frac{3}{4}r + \frac{1}{4}r^2 + \frac{3}{4}r^3 - \frac{1}{2}r^4\Big) \tag{41}$$

and

$$U55 = \Big(-\frac{1}{8}r + \frac{3}{8}r^2 - \frac{3}{8}r^3 + \frac{1}{8}r^4\Big). \tag{42}$$

The effective amplification factor, EAF of LWLF2 is computed as $\Big(|\xi_{LW}|\ |\xi_{LF}|\Big)^{\frac{1}{2}}$ which is equal to

$$\Big((1-2r^2\sin^2(\frac{w}{2}))^2 + (r\ \sin(w))^2\Big)^{1/4}\ \Big(\frac{1}{2}\ (1+\cos(w)+r^2\ (\cos(w)-1))^2 + (r\sin(w))^2\Big)^{1/4}. \tag{43}$$

The effective amplification factor of the LWLF2 scheme after two time steps is calculated as

$$\xi^2 = \Big(1 - 2\ r^2\ \sin^2\Big(\frac{w}{2}\Big) - I\ r\ \sin(w)\Big)\ \times$$
$$\Big[\frac{1}{2}\ (1 + \cos(w) + r^2\ (\cos(w) - 1)) - I\ r\ \sin(w)\Big]. \tag{44}$$

The RPE of the LWLF2 is obtained as $-\frac{1}{2\ rw}\arg(\xi^2)$.

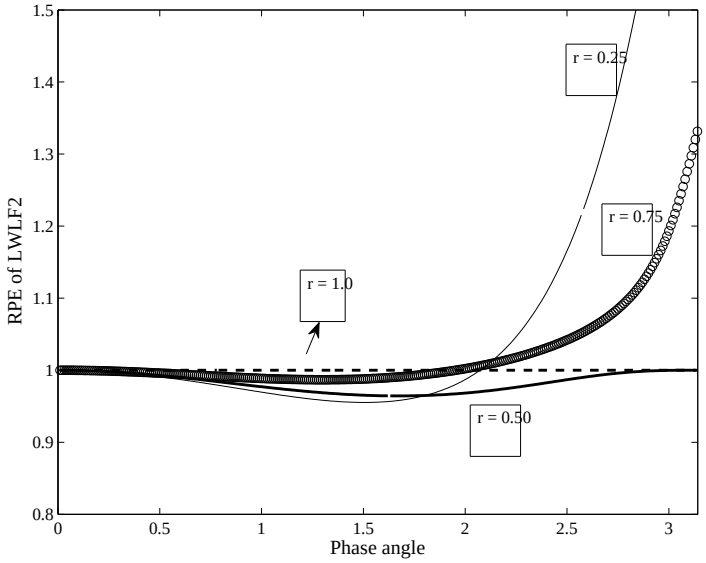

Figure 1: Dependence of relative phase error per unit time step on phase angle for LWLF2 scheme in 1D.

The modified equation of the LWLF2 is

$$u_t + \beta u_x + \frac{1}{8}\Big(-\frac{h^2}{k} + \beta^2 k\Big)u_{xx} + \frac{7}{24}\Big(\beta h^2 - \beta^3 k^2\Big)u_{xxx} + ... = 0, \tag{45}$$

and we can observe that the leading error terms are dissipative in nature. Also, the coefficient of the dissipative term is half that of the Lax-Friedrichs scheme.
A plot of the relative phase error vs phase angle is shown in Fig. (1) at 4 different CFL numbers. At CFL 1, we have null dispersion.

6.4 A linear combination of Lax-Wendroff and the two-step Lax-Friedrichs scheme

We consider a linear combination of Lax-Wendroff and the two-step Lax-Friedrichs scheme in the ratio $\alpha : 1 - \alpha$. The Lax-Wendroff and MacCormack schemes are equivalent schemes when used to discretise the 1D linear advection equation. Consequently, a composite scheme made up of a linear combination of Lax-Wendroff and Lax-Friedrichs schemes in the ratio $\alpha : 1 - \alpha$ is equivalent to a composite scheme made up of a linear combination of MacCormack and Lax-Friedrichs scheme in the ratio $\alpha : 1 - \alpha$.

$$u_i^{n+1} = \alpha\Big(u_i^n - \frac{r}{2}(u_{i+1}^n - u_{i-1}^n) + \frac{r^2}{2}(u_{i+1}^n - 2u_i^n + u_{i-1}^n)\Big)$$
$$+(1-\alpha)\Big(\frac{1}{4}(u_{i-1}^n + 2u_i^n + u_{i+1}^n) - \frac{r}{2}(u_{i+1}^n - u_{i-1}^n) + \frac{1}{4}(u_{i+1}^n - 2u_i^n + u_{i-1}^n)\Big). \quad (46)$$

This scheme is optimised when $\alpha = 0.66$ [3]. If we replace α by 0.66, we get the following method

$$u_i^{n+1} = (0.83 - 0.83r^2)u_i^n + (0.085 - 0.5r + 0.415r^2)u_{i+1}^n + (0.085 + 0.5r + 0.415r^2)u_{i-1}^n. \quad (47)$$

The method is termed as LW+LF.
Using the Von-Neumann Stability Analysis, we obtain the amplification factor as

$$\xi_{LW+LF} = 0.83 - 0.83r^2 + (0.17 + 0.83r^2)(\cos(w) - Ir\sin(w)) \quad (48)$$

The region of stability is $0 < r \leq 1$.
The relative phase error is calculated as

$$RPE_{LW+LF} = -\frac{1}{rw}\tan^{-1}\Big(\frac{\Im\xi_{LW+LF}}{\Re\xi_{LW+LF}}\Big), \quad (49)$$

which yields

$$RPE_{\xi_{LW+LF}} = \frac{1}{rw}\tan^{-1}\Big(\frac{r\sin(w)}{0.83 - 0.83\ r^2 + (0.17 + 0.83\ r^2)\cos(w)}\Big). \quad (50)$$

A plot of the relative phase error of the composite scheme made up of the linear combination of LW and LF vs phase angle for some different values of CFL is shown in Fig. (2) and we observe that at CFL 0.25 and 0.50, the scheme is afflicted by phase lag. At CFL 1, there is no dispersion error and there is both phase lead and phase lag at CFL 0.75.

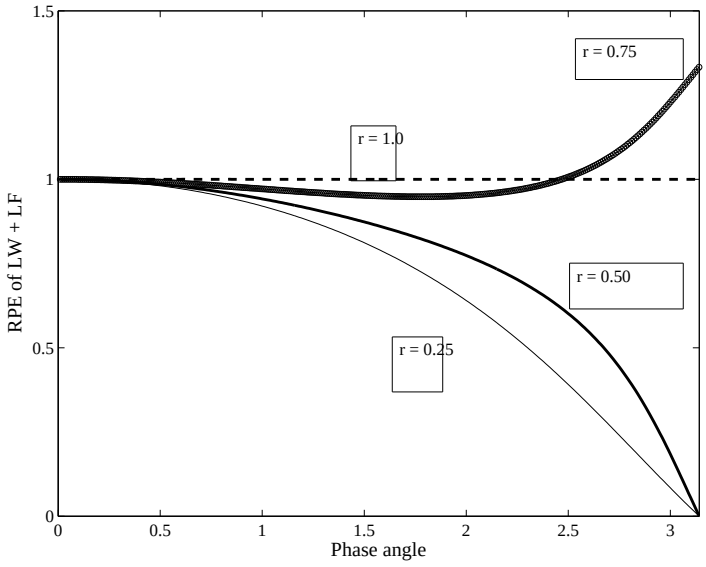

Figure 2: Dependence of relative phase error per unit step on phase angle for LW+LF scheme in 1D.

The modified equation of the LW+LF scheme is given by

$$u_t + \beta u_x + 0.085\ \Big(- \frac{h^2}{k} + \beta^2 k \Big) u_{xx} + \frac{\beta}{6}(h^2 - \beta^2 k^2) u_{xxx} + ... = 0, \tag{51}$$

and we observe that the coefficient of the dissipative term, u_{xx} is less than that of the LWLF2 scheme. Also, the coefficient of the dispersive term, u_{xxx} is less than in LWLF2.

6.5 Fromm's Scheme in 1-D

The Fromm's scheme of zero-average phase error in 1-D [10] uses an average of Lax-Wendroff (LW) and the Beam Warming (BW) schemes. The BW method has a predominantly leading phase error for $0 < r \leq 1$ and a predominantly lagging phase error for $1 < r \leq 2$ [23].
We next obtain a single expression for the Fromm's scheme when applied to the 1D linear advection equation. We first consider the LW and BW schemes which are given by

$$u_i^{n+1} = \frac{1}{2}(r^2 - r)\ u_{i+1}^n + (1 - r^2)\ u_i^n + \frac{1}{2}(r^2 + r)\ u_{i-1}^n, \tag{52}$$

and

$$u_i^{n+1} = u_i^n - \frac{r}{2}\ (3\ u_i^n - 4\ u_{i-1}^n + u_{i-2}^n) + \frac{r^2}{2}\ (u_i^n - 2\ u_{i-1}^n + u_{i-2}^n) \tag{53}$$

respectively.
Then, the Fromm's scheme is obtained as

$$u_i^{n+1} = \frac{r}{4}(r-1)\ u_{i-2}^n + \frac{r}{4}(5-r)\ u_{i-1}^n + \Big(1 - \frac{3r}{4} - \frac{r^2}{4}\Big)\ u_i^n + \frac{1}{4}(r^2 - r)\ u_{i+1}^n. \tag{54}$$

The amplification factor is given by

$$\xi_{Fromm} = 1 - \frac{r}{2}\ (\cos(w) - 1)^2 - \frac{1}{2} r^2\ \sin^2 w + I\ \Big(\frac{1}{2} r^2 \sin(w)(1 - \cos(w)) + \frac{r}{2} \sin(w)(\cos(w) - 3)\Big). \tag{55}$$

The region of stability of Fromm's scheme is obtained as $0 < r \leq 1$.
The relative phase error of the Fromm's scheme is given by

$$RPE_{Fromm's} = -\frac{1}{rw} \tan^{-1} \frac{\Im(\xi_{Fromm})}{\Re(\xi_{Fromm})}. \tag{56}$$

A plot of the RPE vs phase angle, at some different values of CFL is shown in Fig. (3).

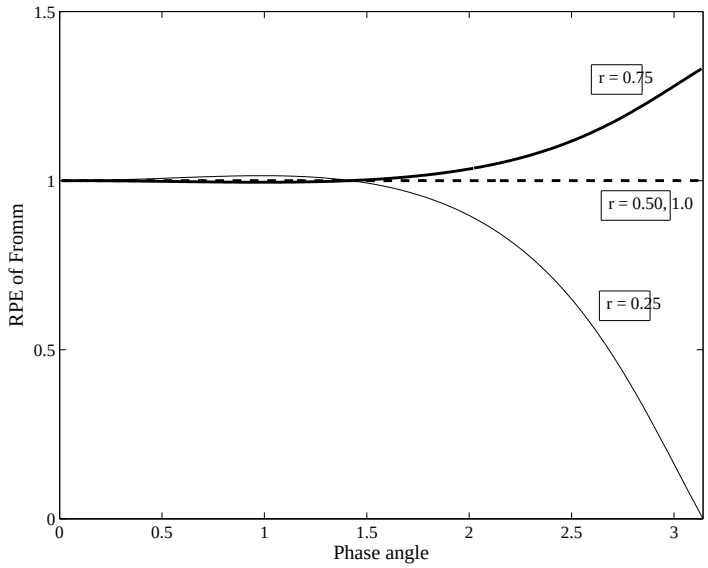

Figure 3: Dependence of the relative phase error per unit time step on phase angle for the Fromm's scheme in 1-D.

The Fromm's scheme has zero dispersion error for all phase angles, $w \in [0, \pi]$ at CFL 0.5 and 1.0. At CFL 0.25, we have mainly phase lag behaviour while at CFL 0.75, phase lead behaviour is dominant, especially at large phase angles.

The modified equation is

$$u_t + \beta u_x - \Big(\frac{\beta h^2}{12} - \frac{\beta^2 hk}{4} + \frac{k^2\beta^3}{6}\Big)u_{xxx} + ... = 0, \tag{57}$$

and we can deduce that the scheme is second order in both time and space.

7 Technique of MIEELDLD

In this section, we describe briefly the techniques of Minimized Integrated Error for Low Dispersion and Low Dissipation **(MIELDLD)** and the Minimized Integrated Exponential Error for Low Dispersion and Low Dissipation **(MIEELDLD)**. These techniques have been introduced in [2]. We now give a resume of how we have derived these techniques.
The Integrated Error for Low Dispersion and Low Dissipation, **IELDLD** is given by

$$\mathbf{IELDLD} = \int_0^{w_1} \mathbf{eldld}\ dw, \tag{58}$$

where

$$\mathbf{eldld} = ||1 - RPE| - (1 - AFM)| + ||1 - RPE| + (1 - AFM)|, \tag{59}$$

and w_1 is a constant.
The Integrated Exponential Error for Low Dispersion and Low Dissipation, **IEELDLD** is described by

$$\mathbf{IEELDLD} = \int_0^{w_1} \mathbf{eeldld}\ dw, \tag{60}$$

where

$$\textbf{eeldld} = \exp\left(\Big||1-RPE|-(1-AFM)\Big|\right) + \exp(|1-RPE|+(1-AFM)) - 2.0, \quad (61)$$

and w_1 is a constant. The measures **eldld** and **eeldld** denote the Error for Low Dispersion and Low Dissipation and Exponential Error for Low Dispersion and Low Dissipation.
For a stable numerical scheme, the dispersion and dissipation errors are calculated as $|1 - RPE|$ and $(1 - AFM)$ respectively.
We now explain briefly how we have devised the concept of **MIEELDLD** as a technique to control dissipation and dispersion in numerical schemes.
For a scheme to have Low Dispersion and Low Dissipation, we require

$$|1-RPE|+(1-AFM) \longrightarrow 0.$$

Also when dissipation neutralises dispersion optimally, we have,

$$\Big||1-RPE|-(1-AFM)\Big| \rightarrow 0.$$

Thus on combining these two conditions, we get the following condition necessary for dissipation to neutralise dispersion and for Low Dispersion and Low Dissipation character to be satisfied:

$$\textbf{eldld} = \Big||1-RPE|-(1-AFM)\Big| + (|1-RPE|+(1-AFM)) \longrightarrow 0. \quad (62)$$

Similarly, we expect

$$\textbf{eeldld} = \exp\left(\Big||1-RPE|-(1-AFM)\Big|\right) + \exp(|1-RPE|+(1-AFM)) - 2 \longrightarrow 0, \quad (63)$$

in order for Low Dispersion and Low Dissipation properties to be achieved.
Figs. (4(a)) and (4(b)) show the plots of the measures of errors namely **eldld** and **eeldld**, both vs RPE vs AFM. It is seen that both **MIELDLD** and **MIEELDLD** are reliable techniques of optimisation to control dispersion and dissipation because when there is null dissipation error and null dispersion error, both measures of error are equal to zero. We note that **eeldld** is comparatively more sensitive to changes in RPE and AFM than **eldld**. Therefore, **MIEELDLD** is more appropriate to measure the control and balance of dispersion and dissipation as it is more sensitive to slight perturbations.

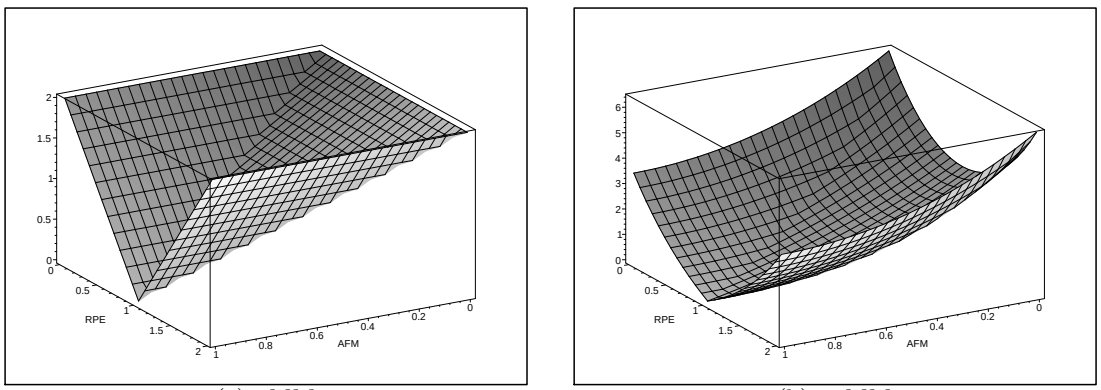

(a) **eldld** (b) **eeldld**

Figure 4: Plot of **eldld** and **eeldld**, both with respect to $RPE \in [0, 2]$ and with respect to $AFM \in [0, 1]$

We next explain how the integration process is performed in order to obtain the optimal parameter for instance the CFL number.
If the CFL number is the only parameter, we compute

$$\int_0^{1.1} \textbf{eeldld}\ dw,$$

and this integral will be a function of r. The optimal CFL is the one at which the integral quantity is closest to zero.

Considerable and extensive work on the technique of Minimised Integrated Exponential Error for Low Dispersion and Low Dissipation has been carried out in [2, 3, 4, 5, 6].
In [2], we have obtained the optimal CFL of some explicit methods like Lax-Wendroff, Beam-Warming and Upwind Leap-Frog when applied to the 1D linear advection equation. In [3], we use the technique to understand why not all composite methods can be effective to control numerical dispersion and dissipation in regions of shocks. In [4], we consider the family of third-order methods proposed by Takacs [20] and we optimize the two parameters for efficient shock-capturing. In [5], we use the technique to construct high-order low dispersion and low dissipation spatial and temporal discretization schemes in Computational Aeroacoustics. Also, in a recent work [6], we optimize a third order Weighted Essentially Non-Oscillatory scheme for 1D hyperbolic conservation laws.

8 Other techniques of Optimisation

Tam and Webb [21], Bogey and Bailly [8] and Berland et al. [9] have implemented techniques which enable coefficients to be determined in numerical schemes specifically designed for Computational Aeroacoustics. We have developed these techniques into respective equivalent forms to determine the optimal CFL for some known numerical schemes in [3].
We now describe briefly how Tam and Webb, Bogey and Bailly and Berland et al. define their measures and consequently their technique of optimisation in Computational Aeroacoustics.
The Dispersion-Relation-Preserving (DRP) scheme was designed so that the dispersion relation of the finite difference scheme is formally the same as that of the original partial differential equations. The integrated error is defined as

$$E = \int_{-\eta}^{\eta} |\theta^* h - \theta h|^2\ d(\theta h),$$

where the quantities $\theta^* h$ and θh represent the numerical and exact wavenumbers respectively. The dispersion error and dissipation error are calculated as $|\Re(\theta^* h) - \theta h|$ and $|Im(\theta^* h)|$ respectively.

Tam and Shen [22] set η as 1.1 and optimise the coefficients in the numerical scheme such that the integrated error is minimised.
Bogey and Bailly [8] minimise the relative difference between the exact wavenumber, θh and the effective/numerical wavenumber, $\theta^* h$ and define their integrated errors as

$$E = \int_{(\theta h)_l}^{(\theta h)_h} \frac{|\theta^* h - \theta h|}{\theta h}\ d(\theta h), \tag{64}$$

or

$$E = \int_{\ln\ (\theta h)_l}^{\ln\ (\theta h)_h} |\theta^* h - \theta h|\ d(\ln\ (\theta h)). \tag{65}$$

We next describe how the optimisation has been performed by Berland et al. [9]. To ensure a minimum order of accuracy, the terms of the Taylor series are cancelled up to fourth order. The coefficients are determined by minimising the integral error which is computed as

$$\int_{\pi/16}^{\pi/2} \Big((1-\alpha)\ |\theta h - Re(\theta^* h)| + \alpha |Im(\theta^* h)| \Big)\ \frac{d(\theta h)}{\theta h}.$$

The value of α chosen where $\alpha \in (0,1)$, depends on the numerical scheme. The bounds of the integral have been arbitrarily chosen to optimise wavenumbers between $\theta h = \dfrac{\pi}{16}$ (32 points/wavelength) and $\theta h = \dfrac{\pi}{2}$ (corresponding to 4 points/wavelength). Fourth-order seven- and eleven-point non-centred finite difference schemes have been designed using this technique.

In Computational Fluid Dynamics for a particular method under consideration, the dispersion error is calculated as

$$|1 - RPE|$$

while the dissipation error as

$$(1 - AFM).$$

We have modified the measures used by Tam and Webb, Bogey and Bailly, Berland et al. in a Computational Aeroacoustics framework to suit them in a Computational Fluid Dynamics framework such that the optimal CFL of some known numerical methods can be obtained [3]. Thus, we define the following integrals: Integrated Error from Tam and Webb, **(IETAM)**, Integrated Error from Bogey and Bailly **((IEBOGEY)** and Integrated Error from Berland et al **(IEBERLAND)** as follows:

$$\mathbf{IETAM} = \int_0^{w_1} \mathbf{ETAM}\ dw, \tag{66}$$

$$\mathbf{IEBOGEY} = \int_0^{w_1} \mathbf{EBOGEY}\ dw, \tag{67}$$

and

$$\mathbf{IEBERLAND} = \int_0^{w_1} \mathbf{EBERLAND}\ dw, \tag{68}$$

where

$$\mathbf{ETAM} = |1 - RPE|^2,$$

$$\mathbf{EBOGEY} = |1 - RPE|,$$

and

$$\mathbf{EBERLAND} = (1-\alpha)|1 - RPE| + \alpha(1 - AFM).$$

The optimal CFL is obtained by plotting the respective integral with respect to the CFL number and locating the CFL at which the integral is least. The techniques used to obtain the quantities **IETAM**, **IEBOGEY** and **IEBERLAND** are defined as Minimised Integrated Error from Tam and Webb **(MIETAM)**, Minimised Integrated Error from Bogey and Bailly **(MIEBOGEY)** and Minimised Integrated Error from Berland et al. **(MIEBERLAND)** respectively [3].

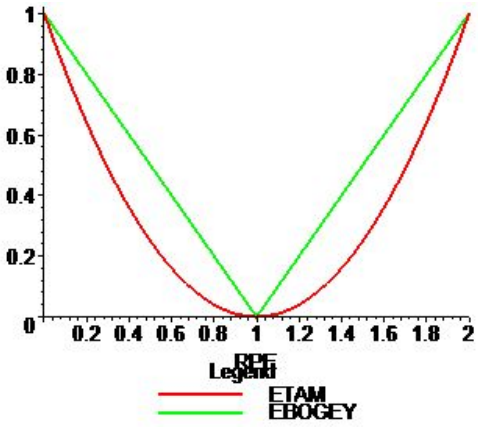

Figure 5: Plot of the measures: **ETAM** and **EBOGEY**, both with respect to $RPE \in [0, 2]$.

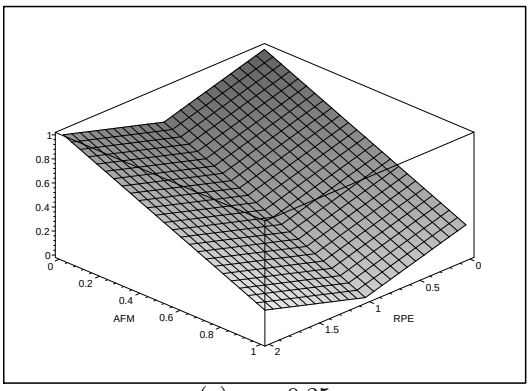

(a) $\alpha = 0.25$

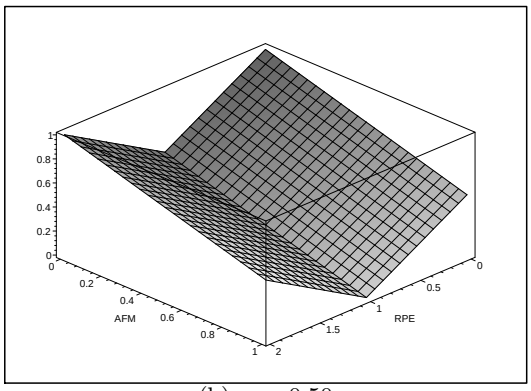

(b) $\alpha = 0.50$

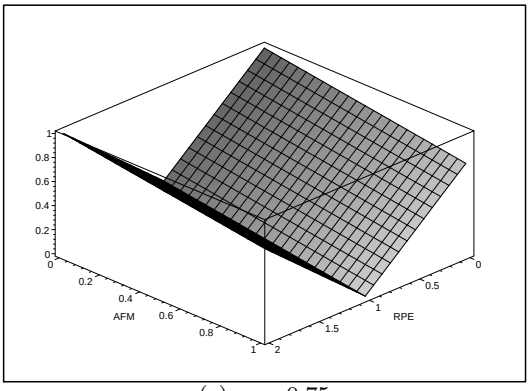

(c) $\alpha = 0.75$

Figure 6: Variation of the quantity, **EBERLAND** vs $AFM \in [0, 1]$ vs $RPE \in [0, 2]$ at different values of α: 0.25, 0.50 and 0.75.

8.1 Variation of Integrated Errors with respect to CFL number

In this section, we compare the variation of the five integrated errors, namely **IETAM**, **IEBOGEY**, **IEBERLAND**, **IELDLD** and **IEELDLD** vs the CFL number for three schemes namely; LWLF2, LW+LF and Fromm's schemes when the latter are used to discretise the 1D linear advection equation.

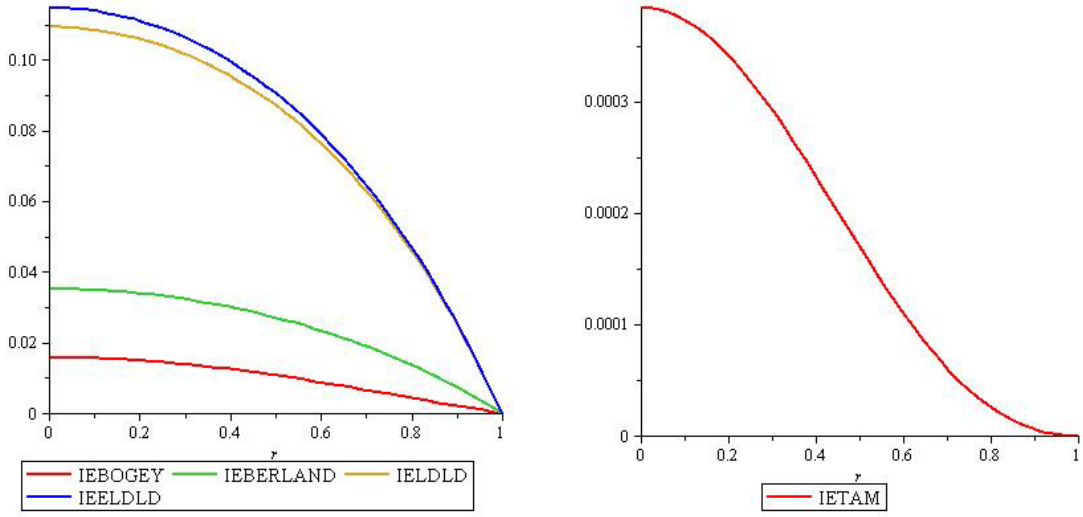

(a) (b)

Figure 7: Variation of integrated errors vs CFL number for the LWLF2 scheme.

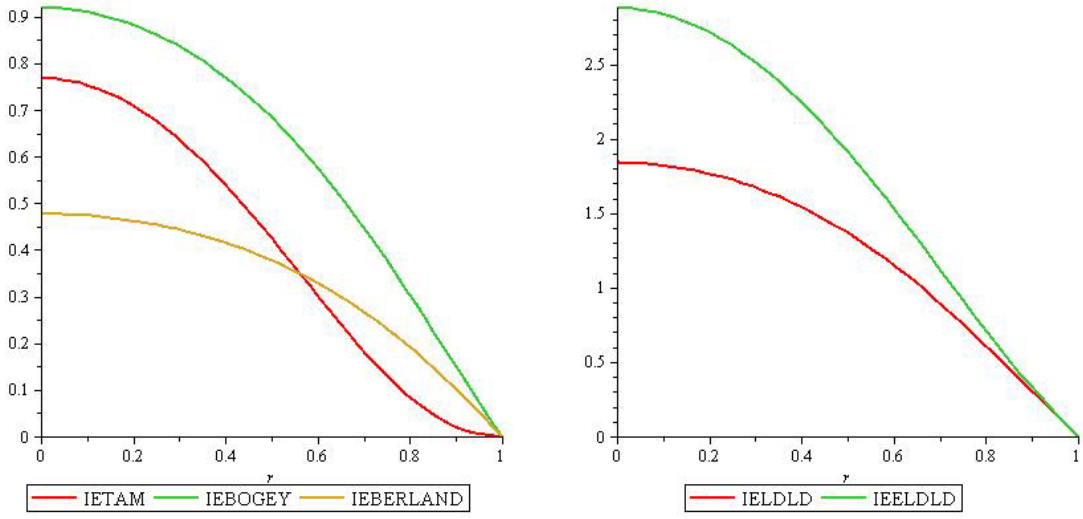

(a) (b)

Figure 8: Variation of integrated errors vs CFL number for the optimised composite scheme made up of a linear combination of Lax-Wendroff and Lax-Friedrichs in the ratio 0.66 : 0.34.

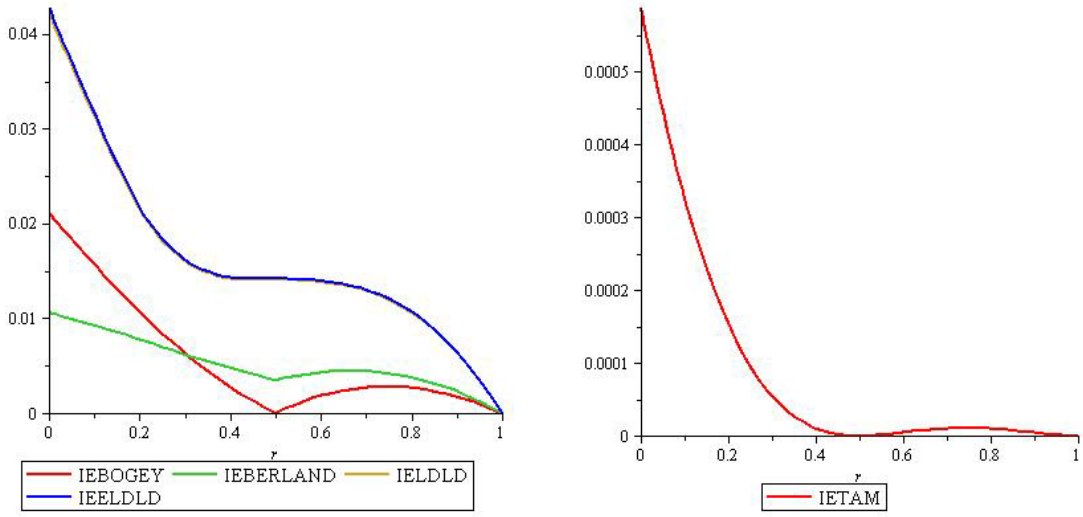

(a) (b)

Figure 9: Variation of integrated errors vs CFL number for the Fromm's scheme.

Fig. (7) shows the variation of the integrated errors vs the CFL number and in all cases, we observe from the graphs that the optimal CFL is 1.0. We have also used the NLPSolve function in Maple and obtain the optimal CFL as 1.0. Indeed the LWLF2 scheme gives exact results at CFL 1.0.
Fig. (8) shows the variation of the integrated errors vs the CFL number for the optimised composite scheme made up of a linear combination of MC and LF schemes. The optimal CFL is 1.0 in all cases. This is seen clearly from the graphs and also on performing a numerical optimization from Maple, we get the optimal CFL as 1.0.
Fig. (9) shows the variation of the integrated errors vs the CFL number and only the measures **IELDLD** and **IEELDLD** give the correct optimal CFL which is 1.0. The measures, **IETAM** and **IEBOGEY** give two optimal CFL namely 0.5 and 1.0. However, it is known that the Fromm's scheme gives exact results only when its CFL is 1.0. On using the NLPSolve function in Maple we obtain the optimal CFL as 0.500000 and 1.000000 on using **IETAM** and **IEBOGEY** respectively.
Hence, we conclude that optimisation techniques based on dispersion alone might not appropriate to compute optimal parameters for efficient shock-capturing based on the 1D linear advection equation.

9 Numerical results for Boxcar function

The results of Boxcar propagation using Lax-Wendroff scheme at four different values of CFL at dimensionless time, $t = 400$ are shown are Fig. (10). Exact results are obtained at CFL 1.0 but at other CFL numbers, the results are dispersive and we observe phase lag.
The results of the Boxcar propagation using the two-step Lax-Friedrichs scheme at 4 different values of CFL at dimensionless time, $t = 400$ are depicted in Fig. (11). The results are highly dissipative at CFL 0.25. At CFL 1.0, we get exact results.
Fig. (12) shows the results of the Boxcar propagation using LWLF2 scheme at four different CFL numbers. At CFL 1.0, we have exact results while at other values of CFL, the results are slightly dissipative.

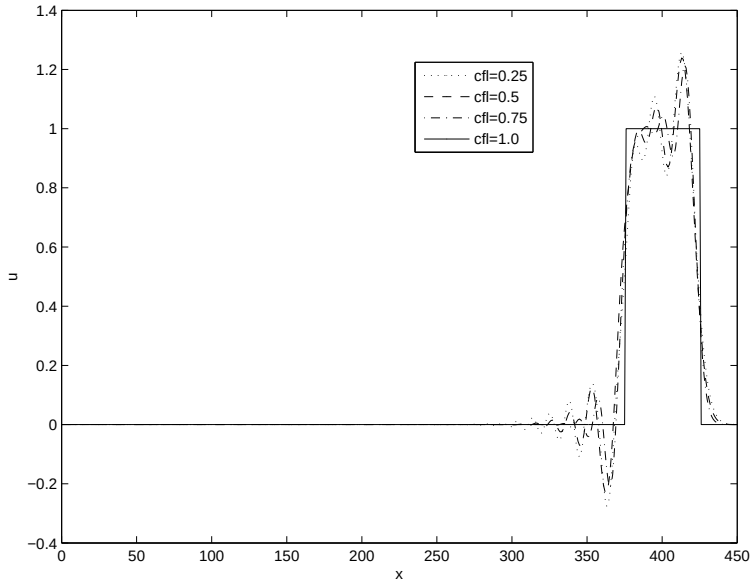

Figure 10: Propagation of boxcar function using the Lax-Wendroff scheme at 4 different CFL numbers: $0.25, 0.5, 0.75, 1.0$ at dimensionless time, $t = 400$.

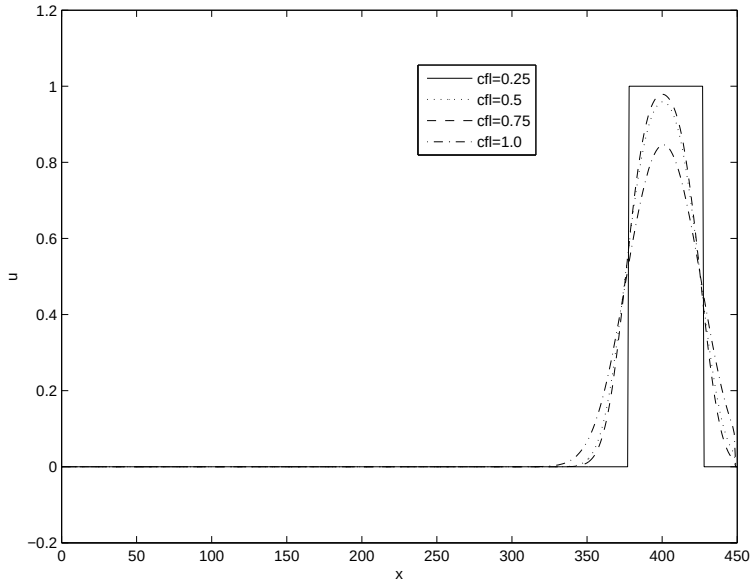

Figure 11: Propagation of boxcar function using the Lax-Friedrichs scheme at 4 different CFL numbers at dimensionless time, $t = 400$.

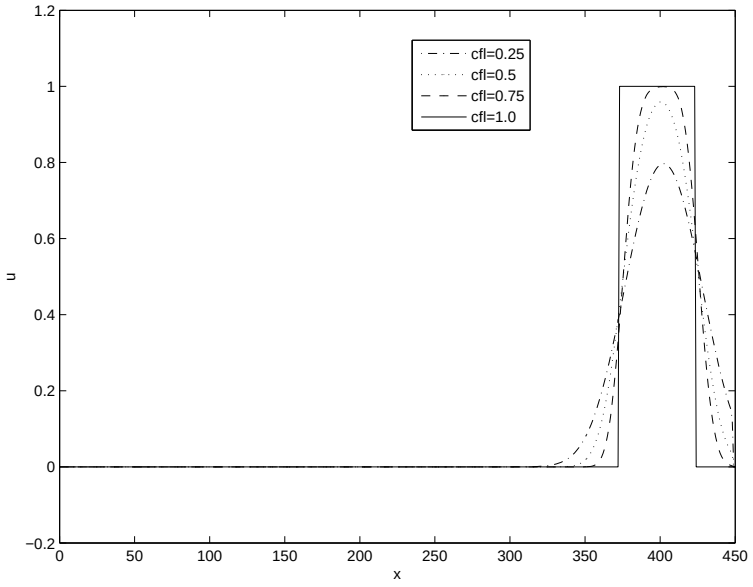

Figure 12: Propagation of boxcar function using LWLF2 scheme at 4 different CFL numbers at dimensionless time $t = 400$.

The results of the Boxcar propagation using the linear combination of the LW and LF schemes at 4 different values of CFL, at dimensionless time, $t = 400$ are shown in Figure (13). The results are dissipative at CFL $0.25, 0.50$ and 0.75. Exact results are obtained at CFL 1.0.

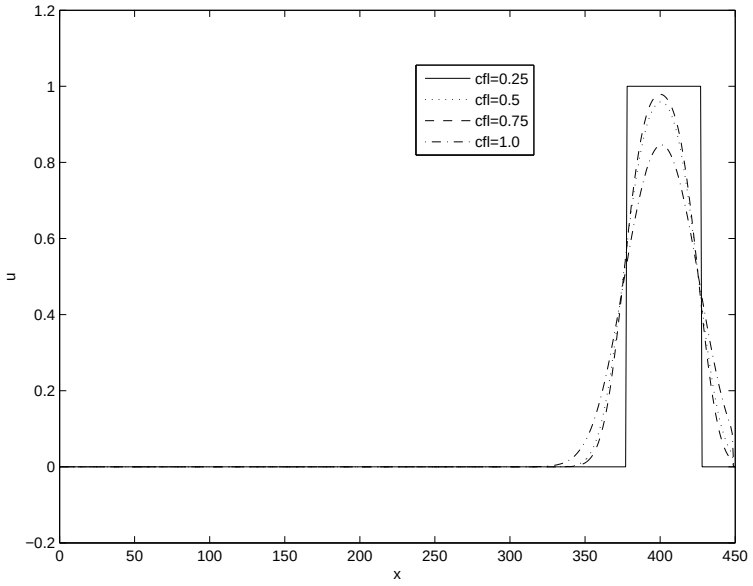

Figure 13: Propagation of boxcar function using the LW+LF scheme at 4 different CFL numbers.

We present the results of the boxcar propagation obtained using the Fromm's scheme in Fig. (14). We observe that we get exact results at CFL 1.0. At other CFL numbers, there are some dispersive oscillations.

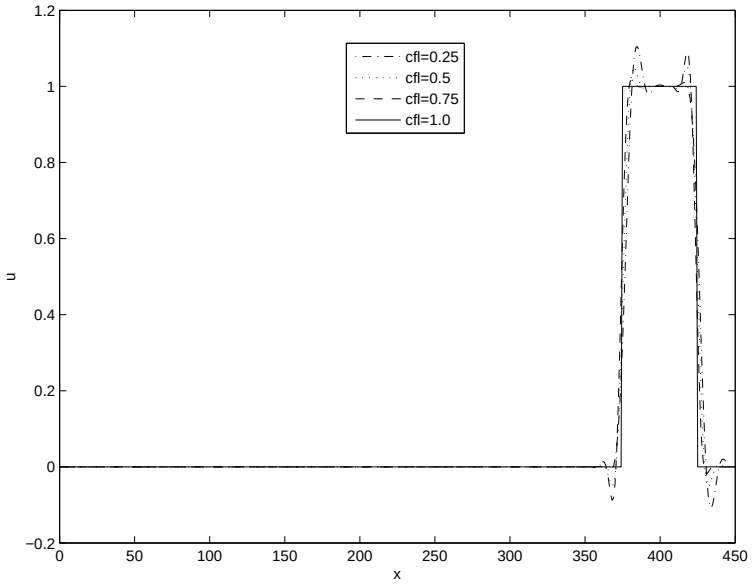

Figure 14: Propagation of boxcar function using the Fromm's scheme at 4 different CFL numbers.

We now tabulate the dissipation error (E_{diss}), dispersion error (E_{disp}), sum of dispersion and dissipation errors and lastly the measure, *eeldld* at some different values of CFL for all the three composite schemes in Tables (1), (2) and (3). These errors are calculated from the numerical results using the technique of Takacs [20], as described in section 4 of the paper.
We also plot the sum of the dispersion and dissipation errors and eeldld vs the CFL number for the three composite methods in Figs. (15), (16) and (17).
Figs. (15) and (16) show the plots of variation of two measures of errors vs the CFL number for LWLF2 and LW+LF schemes. These two measures are the sum of the dispersion and dissipation errors and the quantity, *eeldld*. Both quantities decrease monotonically with increase in CFL number. Figs. (7), (8) show the variation of the five integrated errors vs the CFL number which is monotone decreasing.
Fig. (17) shows the variation of the sum of dispersion and dissipation errors and *eeldld* vs the CFL number for Fromm's scheme. In both cases, the measures show a monotone decreasing behaviour with increase in CFL. Based on Fig. (9), only the integrated error, **IELDLD** and **IEELDLD** show a monotone decreasing behaviour with increase in CFL number. The variation of the integrated errors namely; **IEBOGEY**, **IEBERLAND** and **IETAM** does not mimic the same variation as that of the sum of dispersion and dissipation errors and *eeldld* vs the CFL number in the case of Fromm's scheme.
Hence, we conclude that **IELDLD** and **IEELDLD** are good measures of the shock-capturing properties of numerical schemes approximating the 1D linear advection equation.

Table 1: Errors for the LWLF2 scheme at different CFL numbers for Problem I

CFL	E_{diss}	E_{disp}	Sum of errors	*eeldld*
0.1	1.834×10^{-2}	1.814×10^{-2}	3.648×10^{-2}	3.736×10^{-2}
0.2	9.826×10^{-3}	1.390×10^{-2}	2.372×10^{-2}	2.809×10^{-2}
1/3	5.459×10^{-3}	1.111×10^{-2}	1.656×10^{-2}	2.236×10^{-2}
0.4	4.231×10^{-3}	1.024×10^{-2}	1.447×10^{-2}	2.061×10^{-2}
0.5	2.930×10^{-3}	9.179×10^{-3}	1.211×10^{-2}	1.845×10^{-2}
0.625	1.818×10^{-3}	8.053×10^{-3}	9.871×10^{-2}	1.617×10^{-2}
400/574	1.344×10^{-3}	7.122×10^{-3}	8.466×10^{-3}	1.430×10^{-2}
0.8	7.851×10^{-4}	5.832×10^{-3}	6.617×10^{-3}	1.170×10^{-2}
400/440	3.153×10^{-4}	4.023×10^{-3}	4.338×10^{-3}	8.061×10^{-3}
1.0	0	0	0	0

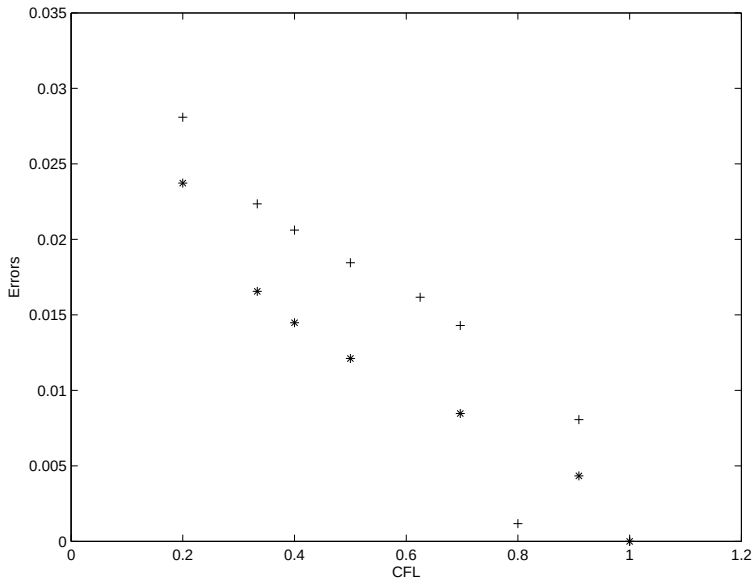

Figure 15: Plot of sum of dispersion and dissipation errors ($* \ * \ *$) and *eeldld* ($+ \ + \ +$) vs CFL number using the LWLF2 scheme for Problem I.

Table 2: Errors for the LW + LF scheme at different CFL numbers for Problem I

CFL	E_{diss}	E_{disp}	Sum of erors	*eeldld*
0.1	1.266×10^{-2}	1.636×10^{-2}	2.901×10^{-2}	3.315×10^{-2}
0.2	6.339×10^{-3}	1.221×10^{-2}	1.855×10^{-2}	2.462×10^{-2}
1/3	3.400×10^{-3}	9.922×10^{-3}	1.332×10^{-2}	1.995×10^{-2}
0.4	2.622×10^{-3}	9.153×10^{-3}	1.118×10^{-2}	1.840×10^{-2}
0.5	1.818×10^{-3}	8.132×10^{-3}	9.950×10^{-3}	1.633×10^{-2}
0.625	1.143×10^{-3}	6.918×10^{-3}	8.061×10^{-3}	1.388×10^{-2}
400/574	8.495×10^{-4}	6.202×10^{-3}	7.052×10^{-3}	1.244×10^{-2}
0.8	5.046×10^{-4}	5.081×10^{-3}	5.586×10^{-3}	1.019×10^{-2}
400/440	2.089×10^{-4}	3.571×10^{-3}	3.780×10^{-3}	7.155×10^{-3}
1.0	0	0	0	0

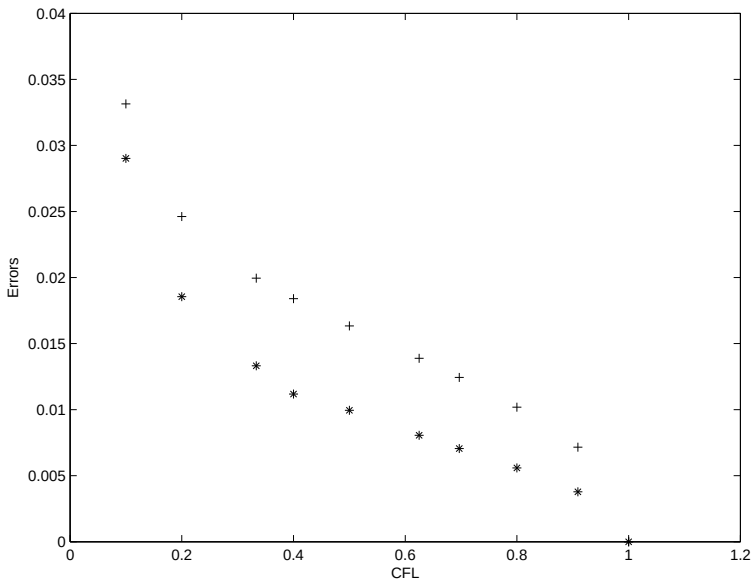

Figure 16: Plot of sum of dispersion and dissipation errors ($* \ * \ *$) and *eeldld* ($+ \ + \ +$) vs CFL number using LW+LF scheme for Problem I.

Table 3: Errors for the Fromm's scheme at different CFL numbers for Problem I

CFL	E_{diss}	E_{disp}	Sum of errors	*eeldld*
0.1	1.068×10^{-4}	4.807×10^{-3}	4.914×10^{-3}	9.638×10^{-3}
0.2	9.352×10^{-5}	4.099×10^{-3}	1.068×10^{-3}	8.216×10^{-3}
1/3	7.799×10^{-5}	3.287×10^{-3}	1.068×10^{-3}	6.585×10^{-3}
0.4	7.103×10^{-5}	2.985×10^{-3}	1.068×10^{-3}	5.980×10^{-3}
0.5	6.137×10^{-5}	2.691×10^{-3}	1.068×10^{-3}	5.389×10^{-3}
0.625	5.012×10^{-5}	2.529×10^{-3}	1.068×10^{-3}	2.579×10^{-3}
400/574	4.373×10^{-5}	2.473×10^{-3}	1.068×10^{-3}	4.952×10^{-3}
0.8	3.409×10^{-5}	2.329×10^{-3}	1.068×10^{-3}	4.664×10^{-3}
400/440	2.171×10^{-5}	1.917×10^{-3}	1.068×10^{-3}	3.837×10^{-3}
1.0	0	0	0	0

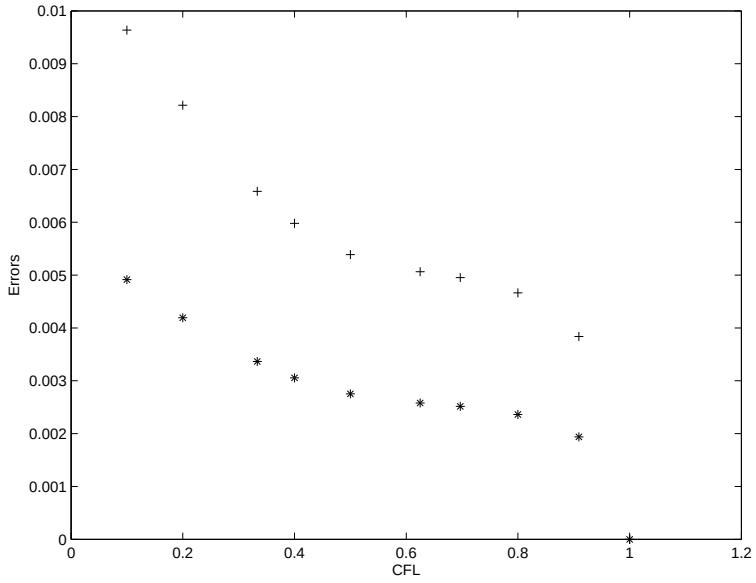

Figure 17: Plot of sum of dispersion and dissipation errors ($* \ * \ *$) and *eeldld* ($+ \ + \ +$) vs CFL number using Fromm's scheme for Problem I.

10 Numerical results for Burger's equation

The results of Problem II using Lax-Wendroff, Lax-Friedrichs, LWLF2 and a composite scheme made up of a linear combination of Lax-Wendroff and Lax-Friedrchs are shown in Figs. (18), (19), (20), (24). The errors are tabulated in Tables (4), (5), (6) and (7). In all these cases, we use a spatial step of 0.01.
The Lax-Wendroff scheme is not a good method to solve numerically the Burger's equation. It gives excessive dispersive oscillations in region of shocks. As the CFL number is increased from 0.1 to 0.8, the results obtained are less worse but at CFL 1.0, the scheme blows up.
The Lax-Friedrichs scheme cause excessive smearing of the shocks at low CFL numbers. But as we increase the CFL, the dissipation errors, dispersion errors, sum of dissipation and dispersion errors and the measure, *eeldld* all decrease. Fig. (21) shows that the sum of dispersion and dissipation errors and *eeldld* all show a monotone decreasing behaviour with increase in CFL number. Quite good results are obtained at CFL 1.0.
The LWLF2 scheme gives in general better results than Lax-Friedrichs. As the CFL number is increased, the results get better. Fig. (22) shows that the sum of dispersion and dissipation errors and *eeldld* all decrease monotonically with increase in CFL number. Best results are obtained at CFl 1.0.
The composite scheme made up of a linear combination of Lax-Wendroff and Lax-Friedrichs is quite a good scheme at specific CFL numbers. At CFL 0.1, 0.2, 0.32, the scheme is quite dissipative. At CFL 0.4 and 0.5, quite good results are obtained. As we increase the CFL to 0.64, 0.8 and 1.0, we have more dispersive oscillations. Fig. (23) show the variation of the sum of the dispersion and dissipation errors and *eeldld* vs the CFL number. They show almost the same variation. Both quantities decrease monotonically as the CFL is increased from 0.1 to 0.4. Then, both quantities increase monotonically as CFL is increased from 0.5 to 1.0. Fig. (24) and Table (7) confirm that best results are obtained at CFL 0.4.

Table 4: Errors for the Lax-Wendroff scheme for Problem II with spatial step 0.01

Time step	CFL	E_{diss}	E_{disp}	Sum of errors	*eeldld*
0.001	0.1	1.306	1.561	2.867	16.877
0.002	0.2	7.571×10^{-1}	1.113	1.870	5.919
0.0032	0.32	5.279×10^{-1}	8.774×10^{-1}	1.405	3.495
0.004	0.4	4.530×10^{-1}	7.893×10^{-1}	1.242	2.863
0.005	0.5	3.889×10^{-1}	7.081×10^{-1}	1.097	2.371
0.064	0.64	3.293×10^{-1}	6.262×10^{-1}	9.555×10^{-1}	1.946
0.080	0.80	2.847×10^{-1}	5.597×10^{-1}	8.444×10^{-1}	1.643
0.01	1.0	unstable	unstable	unstable	unstable

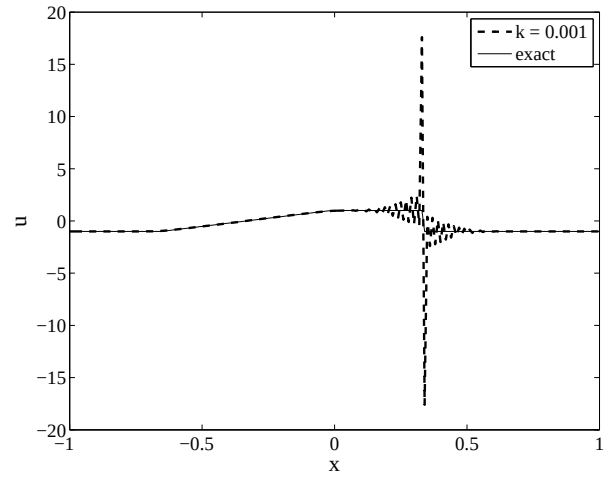

(a)

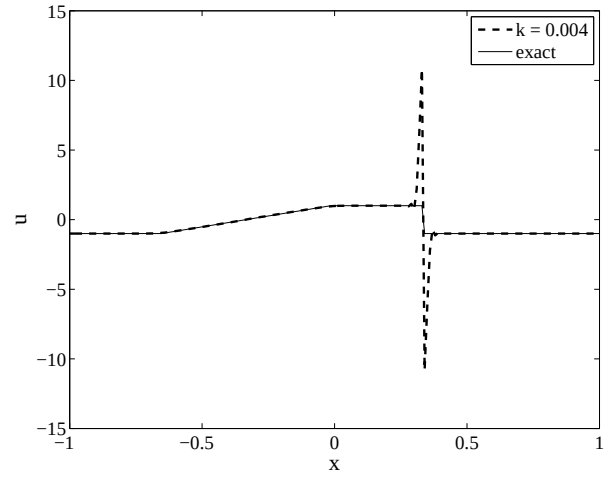

(b)

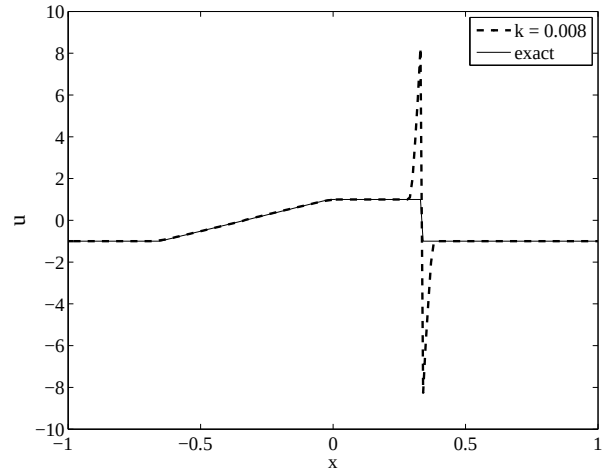

Figure 18: Solutions for Problem II at $T = 0.32$ using Lax-Wendroff scheme at some values of time step.

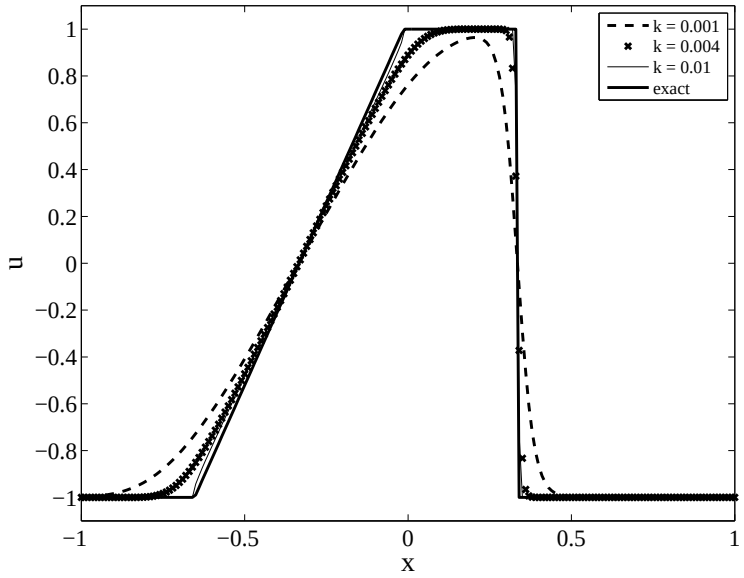

Figure 19: Solutions for Problem II at $T = 0.32$ using Lax-Friedrichs scheme at some values of time step.

Table 5: Errors for the Lax-Friedrichs scheme for Problem II with spatial step 0.01

CFL	E_{diss}	E_{disp}	Sum of errors	*eeldld*
0.1	8.354×10^{-3}	2.066×10^{-2}	2.901×10^{-2}	4.182×10^{-2}
0.2	2.649×10^{-3}	1.107×10^{-2}	1.372×10^{-2}	2.227×10^{-2}
0.32	1.185×10^{-3}	6.764×10^{-3}	7.950×10^{-3}	1.358×10^{-2}
0.4	7.959×10^{-4}	5.195×10^{-3}	5.991×10^{-3}	1.042×10^{-2}
0.5	5.235×10^{-4}	3.861×10^{-3}	4.385×10^{-3}	7.738×10^{-3}
0.64	3.155×10^{-4}	2.614×10^{-3}	2.930×10^{-3}	5.236×10^{-3}
0.80	1.846×10^{-4}	1.684×10^{-3}	1.869×10^{-3}	3.371×10^{-3}
1.0	8.932×10^{-5}	9.797×10^{-4}	1.069×10^{-3}	1.960×10^{-3}

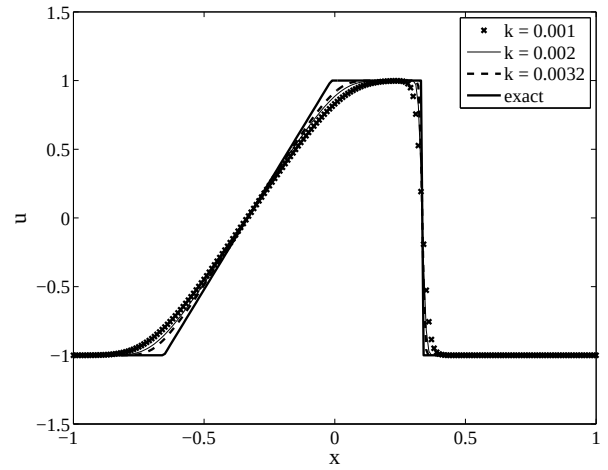

(a)

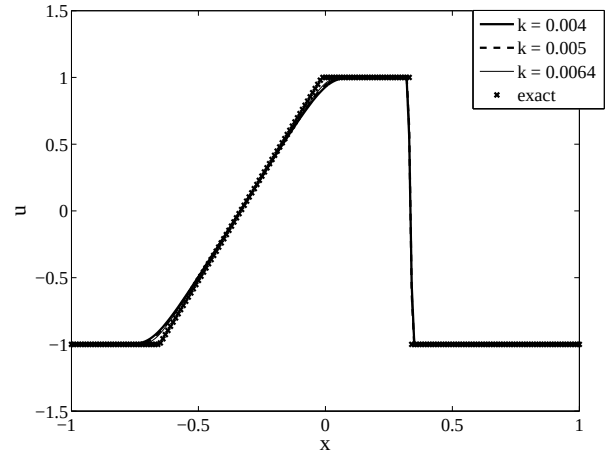

(b)

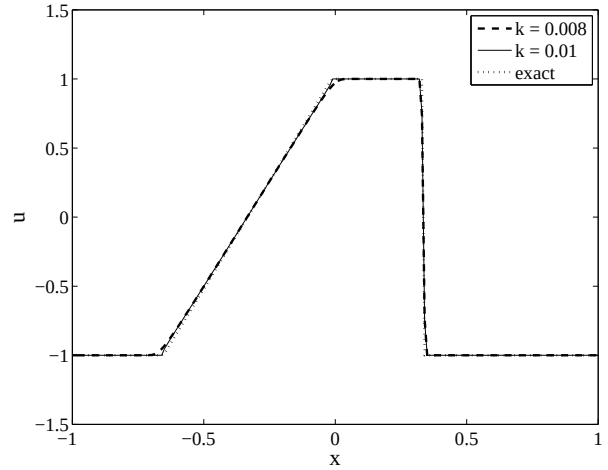

Figure 20: Solutions for Problem II at $T = 0.32$ using LWLF2 scheme at some values of time step.

Table 6: Errors for the LWLF2 scheme for problem II with spatial step 0.01

CFL	E_{diss}	E_{disp}	Sum of errors	*eeldld*
0.1	2.678×10^{-3}	1.122×10^{-2}	1.390×10^{-2}	2.258×10^{-2}
0.2	8.379×10^{-4}	5.549×10^{-3}	6.387×10^{-3}	1.113×10^{-2}
0.32	3.706×10^{-4}	3.193×10^{-3}	3.563×10^{-3}	6.396×10^{-3}
0.4	2.483×10^{-4}	2.362×10^{-3}	2.611×10^{-3}	4.730×10^{-3}
0.5	1.642×10^{-4}	1.693×10^{-3}	1.858×10^{-3}	3.390×10^{-3}
0.64	1.019×10^{-4}	1.142×10^{-3}	1.244×10^{-3}	2.285×10^{-3}
0.80	6.454×10^{-5}	8.184×10^{-4}	8.829×10^{-4}	1.637×10^{-3}
1.0	3.866×10^{-5}	6.899×10^{-4}	7.285×10^{-4}	1.380×10^{-3}

Table 7: Errors for the linear combination of Lax-Wendroff and Lax-Friedrichs scheme for Problem II with spatial step 0.01

CFL	E_{diss}	E_{disp}	Sum of errors	*eeldld*
0.1	1.401×10^{-3}	7.254×10^{-3}	8.654×10^{-3}	1.456×10^{-2}
0.2	4.154×10^{-4}	2.665×10^{-3}	3.081×10^{-3}	5.338×10^{-3}
0.32	1.557×10^{-4}	7.251×10^{-4}	8.808×10^{-4}	1.451×10^{-3}
0.4	8.238×10^{-5}	3.505×10^{-4}	4.329×10^{-4}	7.012×10^{-4}
0.5	3.174×10^{-5}	4.848×10^{-4}	5.165×10^{-4}	9.698×10^{-4}
0.64	4.079×10^{-6}	1.243×10^{-3}	1.247×10^{-3}	2.488×10^{-3}
0.80	1.237×10^{-5}	2.399×10^{-3}	2.411×10^{-3}	4.804×10^{-3}
1.0	6.672×10^{-5}	3.921×10^{-3}	3.988×10^{-3}	7.858×10^{-3}

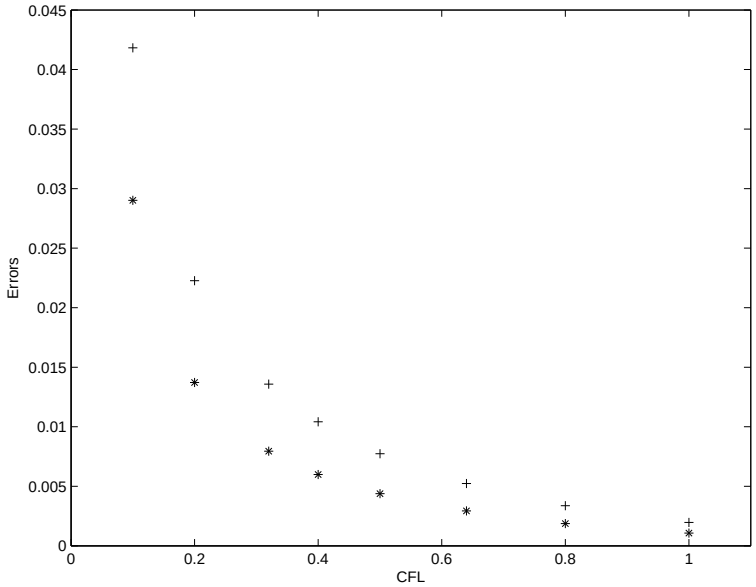

Figure 21: Plot of sum of dispersion and dissipation errors ($* \ * \ *$) and *eeldld* ($+ \ + \ +$) vs CFL number using Lax-Friedrichs scheme for Problem II.

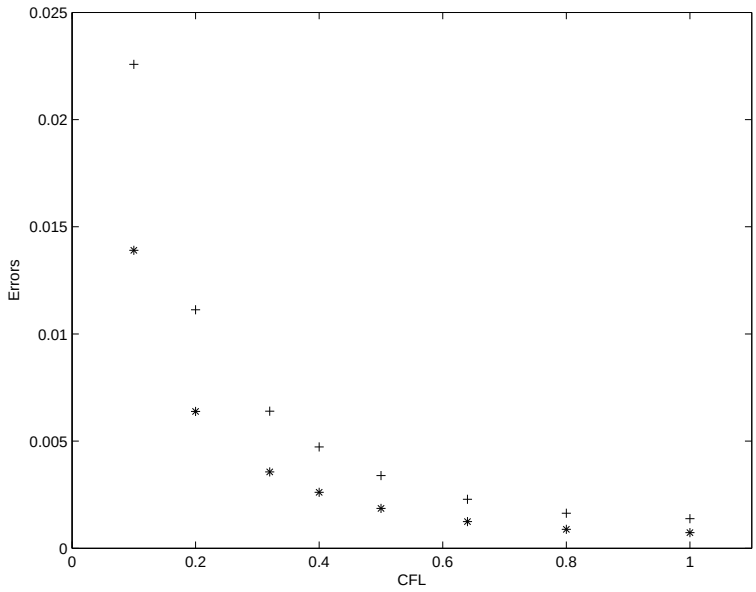

Figure 22: Plot of sum of dispersion and dissipation errors $(* \ * \ *)$ and *eeldld* $(+ \ + \ +)$ vs CFL number using LWLF2 scheme for Problem II.

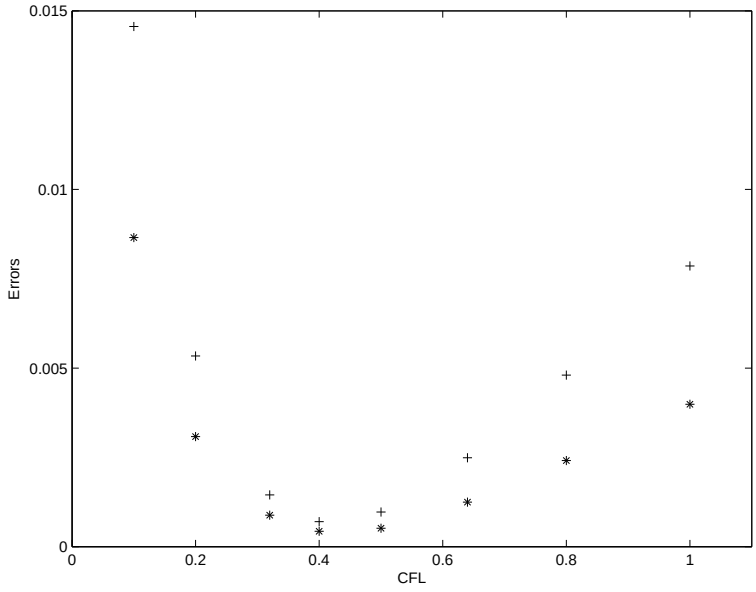

Figure 23: Plot of sum of dispersion and dissipation errors $(* \ * \ *)$ and *eeldld* $(+ \ + \ +)$ vs CFL number using LW+LF scheme for Problem II.

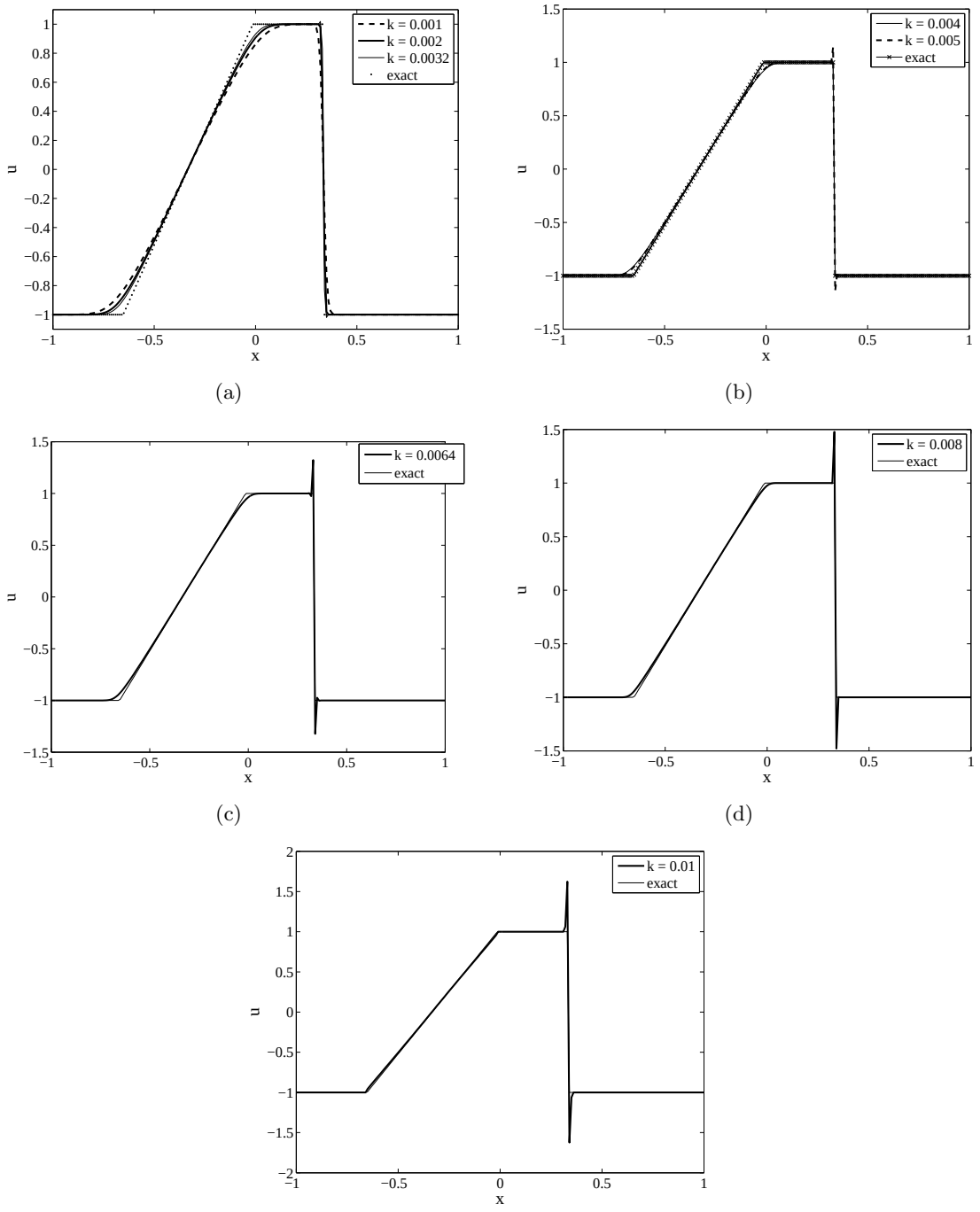

Figure 24: Solutions for Problem II at $T = 0.32$ using a composite scheme made up of a linear combination of Lax-Wendroff and Lax-Friedrichs at some different values of time step.

11 Conclusion

We have used the Lax-Wendroff, Lax-Friedrichs, LWLF2, composite scheme made up of a linear combination of Lax-Wendroff and Lax-Friedrichs (LW+LF) and Fromm's schemes to solve a 1D linear advection equation with initial conditions described by a boxcar function. We observe that out of the five integrated errors, only IELDLD and IEELDLD mimic the variation of the sum of the dispersion and dissipation errors and *eeldld* vs the CFL num-

ber. We note that the measure, **IEBERLAND** which uses a linear combination of sum of dispersion and dissipation erors does not mimic the variation of sum of dispersion and dissipation erors and *eeldld* vs the CFL number.
The Lax-Wendroff, Lax-Friedrichs, LWLF2, LW+LF have also been used to solve Burger's equation subject to some initial and boundary conditions. The LW scheme is not a suitable method as it causes excessive dispersive oscillations in regions of shocks. The LWLF2 scheme gives best results at CFL 1.0 while LW+LF is most effective at CFL close to 0.4. The variation of two quantities namely; sum of dissipation and dispersion errors and *eeldld*, vs CFL number all show a similar variation for the four schemes.

12 Nomenclature

$I = \sqrt{-1}$.
k: time step.
h: spatial step.
β: advection velocity.
r: CFL number.
$r = \dfrac{\beta k}{h}$.
θ: wave number.
w: phase angle.
$w = \theta h$.
n: time level.
RPE: relative phase error.
EAF: Effective Amplification Factor.
IELDLD: Integrated Error for Low Dispersion and Low Dissipation.
MIELDLD: Minimised Integrated Error for Low Dispersion and Low Dissipation.
IEELDLD: Integrated Exponential Error for Low Dispersion and Low Dissipation.
MIEELDLD: Minimised Integrated Exponential Error for Low Dispersion and Low Dissipation.

Acknowledgements
Dr A.R.Appadu is grateful to the Research Development Programme of the University of Pretoria for funding. The period of support is from January 2012 to January 2014. The authors are grateful to the anonymous reviewers for their comments which have helped to improve the quality of the paper substantially.

References

[1] A.R. Appadu, M.Z. Dauhoo and S. D. D. V. Rughooputh, Control of Numerical Effects of Dispersion and Dissipation in Numerical Schemes for Efficient Shock-Capturing Through an Optimal Courant Number, Computers and Fluids. 37 (2008), 767-783.

[2] A.R. Appadu and M.Z. Dauhoo, The Concept of Minimised Integrated Exponential Error for Low Dispersion and Low Dissipation, International Journal for Numerical Methods in Fluids. 65, 5, (2011), 578–601.

[3] A.R. Appadu, Investigating the Shock-Capturing Properties of Some Composite Numerical Schemes for the 1-D Linear Advection Equation, International Journal of Computer Applications in Technology. 43, 2, (2012), 12-27.

[4] A.R. Appadu, Some Applications of the Concept of Minimized Integrated Exponential Error for Low Dispersion and Low Dissipation Schemes, International Journal for Numerical Methods in Fluids. 68, 2, (2012), 244-268.

[5] A.R. Appadu, The Technique of MIEELDLD in Computational Aeroacoustics, Journal of Applied Mathematics, Volume 2012, Article ID 783101, 30 pages.

[6] A.R.Appadu and A.A.I. Peer, Optimized Weighted Essentially Non-Oscillatory Third-Order Schemes for Hyperbolic Conservation Laws, Journal of Applied Mathematics, Volume 2013, Article ID 428681, 12 pages.

[7] R. Babarsky and Robert C. Sharpley, Expanded Stability through Higher Temporal Accuracy for Time-Centred Advection Schemes, Monthly Weather Review. 125, (1997), 1277-1295.

[8] C. Bogey and C. Bailly, A Family of Low Dispersive and Low Dissipative Explicit Schemes for Computing the Aerodynamic Noise, AIAA, (2002).

[9] J. Berland, C. Bogey, O. Marsden and C. Bailly, High-order, Low Dispersive and Low Dissipative Explicit Schemes for Multiple-scale and Boundary Problems, Journal of Computational Physics, 224, (2007), 637-662.

[10] J.E. Fromm, A Method for Reducing Dispersion in Convection Difference Schemes, Journal of Computational Physics, 3, (1968), 179-189.

[11] A. Harten, High Resolutions schemes for Hyperbolic Conservations Laws, Journal of Computational Physics, 49, (1983), 357-393.

[12] Charles Hirsch, Numerical Computation of Internal and External Flows, John Wiley and Sons, 1, (1988).

[13] R. Liska and B. Wendroff, Composite Schemes for Conservation laws, SIAM Journal of Numerical Analysis, 35, (1998), 2250-2271.

[14] Kasahara and Washington, Thermal and Dynamical Effects of Orography on the general circulation of the atmosphere, Proceedings of the WMO/IUGG Symposium on Numerical Weather Predictor, 47-56.

[15] Laney C, Computational Gas Dynamics, Cambridge University Press, Cambridge, 1998.

[16] K. W. Morton and D. F. Mayers, Numerical Solutions for Partial Differential Equations, Cambridge Press, 1994.

[17] A.A.I. Peer, M.Z. Dauhoo, A. Gopaul, M. Bhuruth. A Weighted ENO-flux limiter scheme for hyperbolic conservation laws. International Journal of Computer Mathematics, Vol. 87, No. 15, pp. 3467-3488, 2010.

[18] W. D. Roeck, W. Desmunt, M. Baelmans and P. Sas, An Overview of High-order Finite Differnce Schemes for Computational Aeroacoustics, In Proceedings of ISMA. Katholieke Universiteit Leuven, Belgium (2004). 353-368.

[19] R. Smith and Y. Tang, Optimal and near-optimal advection-diffusion finite difference schemes. V. Error propagation, Proceedings- Royal Society, Mathematical, Physical and Engineering Sciences.

[20] L. Takacs, A Two-Step Scheme for the Advection Equation with Minimized Dissipation and Dispersion errors, Monthly Weather Review. 113, (1985), 1050-1065.

[21] C. K. W. Tam and J. C. Webb, Dispersion-Relation-Preserving Finite Difference Schemes for Computational Acoustics, Journal of Computational Physics. 107, (1993), 262-281.

[22] C. K. W. Tam and H. Shen, Direct Computation of Nonlinear Acoustic pulses using High-order Finite Differences schemes, AIAA 93-4325.

[23] J. C. Tannehill, D. A. Anderson and R. H. Pletcher, Computational Fluid Mechanics and Heat Transfer, Series in Computational and Physical Processes in Mechanics and Thermal Sciences. Taylor and Francis 1997.

[24] H. Trac and U. Pen, A Primer on Eulerian Computational Fluid Dynamics for Astrophysics, Astronomical Society of the Pacific. 115, (2003), 303-321.